THE JOURNAL OF BIOLOGICAL CHEMISTRY VOL. 285, NO. 53, pp. 42115–42129, December 31, 2010

PKCδ Is Activated in a Dietary Model of Steatohepatitis and Regulates Endoplasmic Reticulum Stress and Cell Death*[S]

Received for publication, July 26, 2010, and in revised form, October 20, 2010 Published, JBC Papers in Press, October 22, 2010, DOI 10.1074/jbc.M110.168575

Michael W. Greene[‡1], Christine M. Burrington[‡], Mary S. Ruhoff[‡], Andrew K. Johnson[‡], Tepsiri Chongkrairatanakul[§], and Atipon Kangwanpornsiri[§]

From the [‡]Bassett Research Institute and the [§]Department of Internal Medicine, Bassett Medical Center, Bassett Healthcare Network, Cooperstown, New York 13326

Hepatic steatosis can progress to the clinical condition of non-alcoholic steatohepatitis (NASH), which is a precursor of more serious liver diseases. The novel PKC isoforms δ and ϵ are activated by lipid metabolites and have been implicated in lipid-induced hepatic disease. Using a methionine- and choline-deficient (MCD) dietary model of NASH, we addressed the question of whether hepatic PKCδ and PKCϵ are activated. With progression from steatosis to steatohepatitis, there was activation and increased PKCδ protein content coincident with hepatic endoplasmic reticulum (ER) stress parameters. To examine whether similar changes could be induced *in vitro*, McA-RH 7777 (McA) hepatoma cells were used. We observed that McA cells stored triglyceride and released alanine aminotransferase (ALT) when treated with MCD medium in the presence of fatty acids. Further, MCD medium with palmitic acid, but not oleic or linoleic acids, maximally activated PKCδ and stimulated ER stress. In PKCδ knockdown McA cells, MCD/fatty acid medium-induced ALT release and ER stress induction were completely blocked, but triglyceride storage was not. In addition, a reduction in the uptake of propidium iodide and the number of apoptotic nuclei and a significant increase in cell viability and DNA content were observed in PKCδ knockdown McA cells incubated in MCD medium with palmitic acid. Our studies show that PKCδ activation and protein levels are elevated in an animal model of steatohepatitis, which was recapitulated in a cell model, supporting the conclusion that PKCδ plays a role in ALT release, the ER stress signal, and cell death.

The classical (α, β, and γ), and novel (δ, ϵ, and θ) protein kinase C (PKC) isoforms constitute a set of intracellular signaling molecules that are activated by lipids (1). In fact, the novel PKC isoforms have the highest affinity of all of the PKC isoforms to bind diacylglycerol, a free fatty acid metabolite (2). In agreement with this determination, lipid infusion has been shown to induce muscle and hepatic novel PKC isoform (PKCθ, PKCϵ, and PKCδ) activation but not that of classical or atypical PKC isoforms (3–6). Activation and/or increased expression of novel PKC isoforms have been suggested to play a role in the development of fat-induced pathological conditions. This idea has gained support from studies showing that reduced expression of PKCϵ in the liver and white adipose tissue prevented fat-induced hepatic steatosis (7). Furthermore, high fat diet-induced hyperlipidemia and up-regulation of hepatic genes controlling lipogenesis were found to be reduced in PKCδ null mice (9). These studies and others suggest that novel PKC isoforms play a role in lipotoxicity, with PKCθ being critical in muscle and PKCϵ and PKCδ in liver.

Non-alcoholic fatty liver disease, which is often associated with obesity, is believed to be initiated by the accumulation of lipids in the liver (steatosis), which is considered a benign condition (10, 11). However, hepatic steatosis can progress to the clinical condition of non-alcoholic steatohepatitis (NASH)[2] which is a precursor for more serious liver diseases, such as cirrhosis and hepatocellular carcinoma (10). Although the precise mechanism by which steatosis progresses to NASH is unknown, a "two-hit" hypothesis has been proposed to explain progression (12). Steatosis constitutes the "first hit." Proinflammatory cytokines (*e.g.* TNFα), oxidative stress, and lipid peroxidation constitute the "second hit" leading to NASH (10, 11). A widely used nutritional model of NASH with histological features that most closely resemble those seen in humans is the methionine and choline-deficient (MCD) dietary rodent model (13). Mice or rats fed the MCD diet develop hepatic steatosis, ER stress, induction of the unfolded protein response, focal inflammation, hepatocyte necrosis, and fibrosis (13–15). To determine whether novel PKC isoform activation occurs during the progression from steatosis to NASH, we investigated the temporal relationship of the development of NASH with PKC isoform activation in MCD diet-fed mice. The direct role of one PKC isoform, PKCδ, in the development of free fatty acid- and MCD medium-induced hepatocyte dysfunction and cell death was investigated further in McA-RH7777 (McA) cells. Our results indicate that PKCδ activation plays a role in progression of steatosis to NASH.

* This work was supported by the Stephen C. Clark Fund (to M. W. G.) and the E. Donnall Thomas Resident Research Fund (to A. K. and T. C.).

[S] The on-line version of this article (available at http://www.jbc.org) contains supplemental Figs. 1–5.

[1] To whom correspondence should be addressed: Bassett Research Institute, One Atwell Rd., Cooperstown, NY 13326. Tel.: 607-547-3676; Fax: 607-547-3061; E-mail: michael.greene@bassett.org.

[2] The abbreviations used are: NASH, non-alcoholic steatohepatitis; ALT, alanine aminotransferase; CHOP, C/EBP-homologous protein; eIF2α, eukaryotic translation initiation factor 2α; ER, endoplasmic reticulum; McA, McArdle RH-7777; MCD, methionine- and choline-deficient; PERK, protein kinase-like endoplasmic reticulum kinase; PI, propidium iodide; TBARS, thiobarbituric acid-reactive substances; TG, triglyceride; TMAO, trimethylamine *N*-oxide; Luc, luciferase; mPKC, mouse PKC.

MATERIALS AND METHODS

Animals—Male C57BL/6J mice were housed 4 per cage in Thoren units in the Bassett Research Institute, an AAALAC-accredited animal facility, in light/dark (12 h light/12 h dark), temperature-controlled (22 °C), and humidity-controlled rooms. Mice were provided with standard laboratory chow and water *ad libitum* in accordance with an institutional animal care and use committee-approved protocol. No procedures were undertaken that caused more than minimal pain, distress, or discomfort. Mice were placed on a control (MP Biomedical, catalog no. 960441) or MCD (MP Biomedical, catalog no. 960439) diet for 1–4 weeks. Mice were sacrificed by inhalation of CO_2. Blood samples were immediately drawn from the caudal vena cava. After clotting at room temperature, the sample was centrifuged at 12,000 × *g* for 15 min at 4 °C. The serum was removed and stored frozen at −80 °C until tested. Liver tissue was excised, weighed, and flash frozen in liquid nitrogen or fixed in 10% buffered formalin prior to paraffin embedding.

Histological Analysis of Liver Tissue—Paraffin-embedded sections were stained with hematoxylin and eosin and Masson's trichrome, examined in a blinded fashion by a board certified pathologist, and then graded for steatosis by determining the overall percentage of liver parenchyma containing lipid vacuoles, with 0 = none, 1 = mild (<30%), 2 = moderate (30–60%), and 3 = marked (>60%). Inflammation was graded by the presence or absence of inflammatory cells, with 0 = absent, 1 = minimal or focal occasional single clusters of inflammatory cells present in a few microscopic fields, 2 = mild inflammation, 3 = moderate inflammation, and 4 = marked inflammation. The pattern of fibrosis was graded with 0 = none, 1 = portal fibrosis, 2 = periportal fibrosis or rare septa, 3 = septal fibrosis and architectural distortion but not true cirrhosis, and 4 = cirrhosis, widespread fibrosis, and hepatocyte nodule formation.

Thiobarbituric Acid-reactive Substances (TBARS)—Liver samples were flash frozen and ground in liquid nitrogen. Ground tissue (50–100 mg) was homogenized on ice in buffer containing 0.5 mM BHT, 20 mM Tris, pH 7.4. The homogenate was tested for TBARS (ZeptoMetrix, Buffalo, NY) following the manufacturer's instructions. Protein content was determined by the Coomassie Plus protein assay (Thermo Scientific/Pierce). TBARS units (nmol/ml) were normalized to protein concentration.

Antibodies—Polyclonal antibodies to phospho-PKCδ (Thr^{505}), phospho-PKCδ (Ser^{643}), phospho-PERK (Thr^{980}), JNK1/2, and monoclonal antibodies to phospho-eIF2α (Ser^{51}), phospho-JNK (Thr^{183}/Tyr^{185}), and IRE1α were from Cell Signaling Technology (Danvers, MA). Polyclonal antibodies to PKCδ (C-17), PKCε (C-15), PKCα (C-20), and GADD153 (B-3) (CHOP) and monoclonal antibodies to GAPDH (6C5) were from Santa Cruz Biotechnology, Inc. (Santa Cruz, CA). A polyclonal antibody to calnexin was from Calbiochem/EMD Biosciences (La Jolla, CA). Monoclonal antibodies to α-tubulin and BiP/GRP78 were from Sigma-Aldrich and BD Biosciences, respectively. Goat anti-mouse and anti-rabbit peroxidase-conjugated antibodies were from Sigma-Aldrich. Goat anti-rabbit and anti-mouse Alexa Fluor 635-conjugated secondary antibodies were from Molecular Probes/Invitrogen.

Reagents—DMEM and DMEM-deficient in MCD media were from Invitrogen. Plasmid purification kits were from Qiagen (Valencia, CA). Chemiluminescence detection reagent (ECL Plus) was from GE Healthcare. Palmitic acid, fatty acid-free BSA, and other chemicals were from Sigma-Aldrich. Linoleic and oleic acid were from Cayman (Ann Arbor, MI). The BCA protein assay kit was from Pierce. The lentiviral packaging plasmids, pRRE, pRev, and pMD2G were provided by Didier Trono (Geneva, Switzerland). The lentiviral shRNA plasmid pLKO.1 was provided by Robert Weinberg (Cambridge, MA). Protease inhibitor mixture Set I (100×) and trimethylamine *N*-oxide (TMAO) were from Calbiochem/EMD Biosciences (La Jolla, CA).

Alanine Aminotransferase Assay—The Alanine Aminotransferase-SL Assay (Genzyme Diagnostics) was performed in 96-well plates. The change in absorbance at 340 nm at 37 °C was monitored over 12 min using a Molecular Devices Spectramax spectrophotometer and SOFTmax PRO software. ALT was calculated as units/liter using the manufacturer's formula and molar extinction coefficient of NADH. ALT released into the medium by cultured cells was determined using concentrated conditioned medium. Millipore Amicon centrifugal filters were used to concentrate the conditioned medium 10-fold. Protein content in the cultured cells was determined by the BCA assay. ALT (units/liter) was normalized to protein concentration.

Cell Culture and Treatments—McA rat hepatoma cells were maintained in DMEM containing 10% fetal bovine serum, 10% bovine growth serum, 100 units/ml penicillin, and 100 μg/ml streptomycin (DMEM growth medium) at 37 °C and 5% CO_2. Twenty-four hours after plating, the cells were treated with BSA complexes of 0.4 mM of palmitic, oleic, or linoleic acid or BSA, as indicated. Fatty acids were complexed with fatty acid-free BSA by a method modified from that described by Svedberg *et al.* (16). Briefly, fatty acids in ethanol were added to 0.1 N NaOH to yield 40 mM stocks that were then added to 8% (w/v) BSA in DMEM (control) or MCD culture medium, preheated to 50 °C, to yield BSA conjugated 4 mM fatty acid stocks. The fatty acid-BSA stocks were diluted into DMEM (control) or MCD culture medium to obtain a final concentration of 0.4 mM fatty acid and 0.8% BSA. The pH of all media was adjusted to 7.4, and then they were filter-sterilized prior to use in experiments.

Short term (1–24 h) incubation in MCD medium, which is deficient in choline (an essential nutrient) and methonine (a methyl donor and an essential amino acid), was used in the present studies. It has been shown in long term (24–72 h) culture with medium deficient in choline or methonine that protein and phospholipid synthesis are reduced (17, 18). Long term culture with medium deficient in choline or methonine also results in programmed cell death (17, 18), suggesting that depletion of intracellular pools of methyl group donors and choline moieties is detrimental for long term cell survival.

Lentiviral Infection of McA Cells—PKCδ and luciferase shRNAs and lentiviral production were as previously de-

TABLE 1
Body and liver weights and serum metabolic parameters
Values represent the means ± S.E. for $n = 4–5$. Con, control diet.

	Week 1		Week 2		Week 3		Week 4	
	Con	MCD	Con	MCD	Con	MCD	Con	MCD
Body weight (g)	27.2 ± 1.2	21.0 ± 1.0[a]	29.8 ± 1.0	18.6 ± 0.6[a]	31.0 ± 0.9	17.3 ± 0.6[a]	31.3 ± 0.7	16.7 ± 0.4[a]
Liver weight (g)	1.60 ± 0.06	1.22 ± 0.09[a]	1.58 ± 0.06	1.09 ± 0.04[a]	1.71 ± 0.06	1.02 ± 0.07[a]	1.66 ± 0.05	0.96 ± 0.06[a]
Glucose (mg/dl)	158 ± 18	88 ± 15[a]	171 ± 38	59 ± 11[a]	158 ± 10	55 ± 4[a]	155 ± 35	60 ± 7[a]
Triglyceride (mg/dl)	115 ± 13	60 ± 13[a]	115 ± 12	65 ± 12[a]	91 ± 25	68 ± 17[a]	145 ± 30	63 ± 10[a]
ALT (units/liter)	24 ± 2	232 ± 48[a]	14 ± 3	275 ± 54[a]	20 ± 6	301 ± 40[a]	12 ± 2	216 ± 38[a]

[a] $p < 0.05$ *versus* control diet.

scribed (19, 20). In brief, cells were cultured overnight in DMEM growth medium and then washed and infected with ~100 ng/ml lentivirus in the presence of 5 μg/ml Polybrene for 6 h. Following 16 h in DMEM growth medium, the cells were infected a second time, as described above. Resistant cells were selected using medium containing 20 μg/ml puromycin dihydrochloride.

Subcellular Fractionation—Cells or liver tissue were homogenized by passage through a 25-gauge needle seven or eight times on ice in buffer containing 10 mM Tris, pH 7.4, 20 mM sucrose, 0.1 mM Na_3VO_4, 100 nM okadaic acid, and 1× protease inhibitor mixture. Homogenates were centrifuged at 100,000 × *g* for 30 min at 4 °C. The supernatant was removed and designated as the cytosolic fraction. The pellet was resuspended in buffer containing 10 mM Tris, pH 7.4, 2 mM NaCl, 1% Triton X-100, 0.1 mM Na_3VO_4, 100 nM okadaic acid, and 1× protease inhibitor mixture Set I, incubated on ice for 30 min, and then centrifuged at 100,000 × *g* for 30 min at 4 °C. The resultant supernatant was transferred to a fresh tube and designated as the membrane fraction.

Western Blot Analysis—Cells or liver tissue were lysed with 50 mM Hepes, pH 7.5, 150 mM NaCl, 1% Nonidet P-40, 0.1% SDS, 0.1% sodium deoxycholate, 1 mM NA_3VO_4, 100 nM okadaic acid, and 1× protease inhibitor mixture Set I. Cellular debris was removed by centrifugation at 15,000 rpm for 15 min at 4 °C. Protein content of the clarified lysate was determined by a BCA assay. Isolated proteins were denatured in SDS gel buffer, separated by SDS-PAGE, and immunoblotted. Goat anti-rabbit and anti-mouse Alexa Fluor 635 or HRP-conjugated secondary antibodies were used to detect antibody binding.

Cell Death Analysis—For cell death analysis, McA cells were seeded into 96-well plates at a density of 2×10^4 cells/well and treated without or with MCD medium containing either BSA or 0.4 mM palmitic acid for 24 h. The CellTiter 96® AQ_{ueous} One solution cell proliferation assay kit (Promega Corp., Madison, WI) and the CyQUANT® cell proliferation assay kit (Molecular Probes, Eugene, OR) were used according to the manufacturer's instructions. Three independent experiments were performed with each sample in triplicate. To examine nuclear morphology, cells were grown on glass coverslips and then treated without or with MCD medium containing either BSA or palmitic acid for 24 h. The glass coverslips were gently washed twice with PBS, fixed in a 3.0% formaldehyde solution for 20 min, washed again twice with PBS, and then stained with 50 μM DAPI for 5 min. Coverslips were placed on glass slides with ProLong Gold antifade reagent (Molecular Probes, Inc., Eugene, OR). Results were determined by visual observation of nuclear morphology through fluorescence microscopy. Four separate fields on each slide were analyzed, with a total of at least 250 nuclei being counted. To examine plasma membrane integrity, a quantitative vital dye exclusion assay was performing using propidium iodide (PI). Briefly, McA cells were seeded into 12-well dishes at a density of 2.5×10^5 cells/dish, allowed to adhere for 16 h, and then treated with MCD medium containing either BSA or 0.4 mM palmitic acid for 24 h. During the final 1 h of treatment, PI (10 μg/ml) and Hoechst 33258 (10 μg/ml) were added to the dishes. Cells were washed with PBS, trypsinized, resuspended in PBS, and spun at 500 × *g* for 10 min. The pellet was resuspended in PBS, spun at 500 × *g* for 10 min, washed in PBS, spun at 1000 × *g* for 5 min, and resuspended in PBS. One-tenth of the sample was added to the well of a black 96-well optical plate. The plates were read on a Molecular Devices fmax fluorescent plate reader set to 355 nm excitation/460 nm emission for Hoechst 33258 fluorescence and 544 nm excitation/590 nm emission for PI fluorescence. Values were reported as total PI fluorescence units normalized to total DNA (Hoechst fluorescence).

shRNA Rescue—To establish that a phenotypic change observed in the PKCδ knockdown cells was due to a reduction in PKCδ protein levels, shRNA rescue was performed (21). The mouse PKCδ cDNA was used as a template for multisite-directed mutagenesis using the Stratagene site-directed mutagenesis kit. A primer (5′-CGACATGCCTCATCGGTTTAAAGTGTACAACTACATGAGCCCC-3′) was designed to introduce six silent nucleotide substitutions within the PKCδ shRNA hybridizing sequence (supplemental Fig. 5).

Statistical Analysis—Chemiluminescent and fluorescent signals were directly quantitated using a Storm 860 imager and ImageQuant version 5.1 software. The absolute integration value of the immunoreactive bands minus background was determined. Statistical significance was determined by Student's *t* test ($\alpha = 0.05$) or a one-way repeated measures analysis of variance ($\alpha = 0.05$), using the XLSTAT 2009 program (Addinsoft, New York, NY). Pairwise comparisons were made using Tukey's test ($\alpha = 0.05$).

RESULTS

Time Course of Steatohepatitis in Mice—Mean body and liver weights and serum triglyceride (TG) of mice fed a MCD diet over a 4-week time course were significantly less than in mice fed a control diet over the same time course (Table 1), consistent with previous reports in rodents (13). Serum ALT

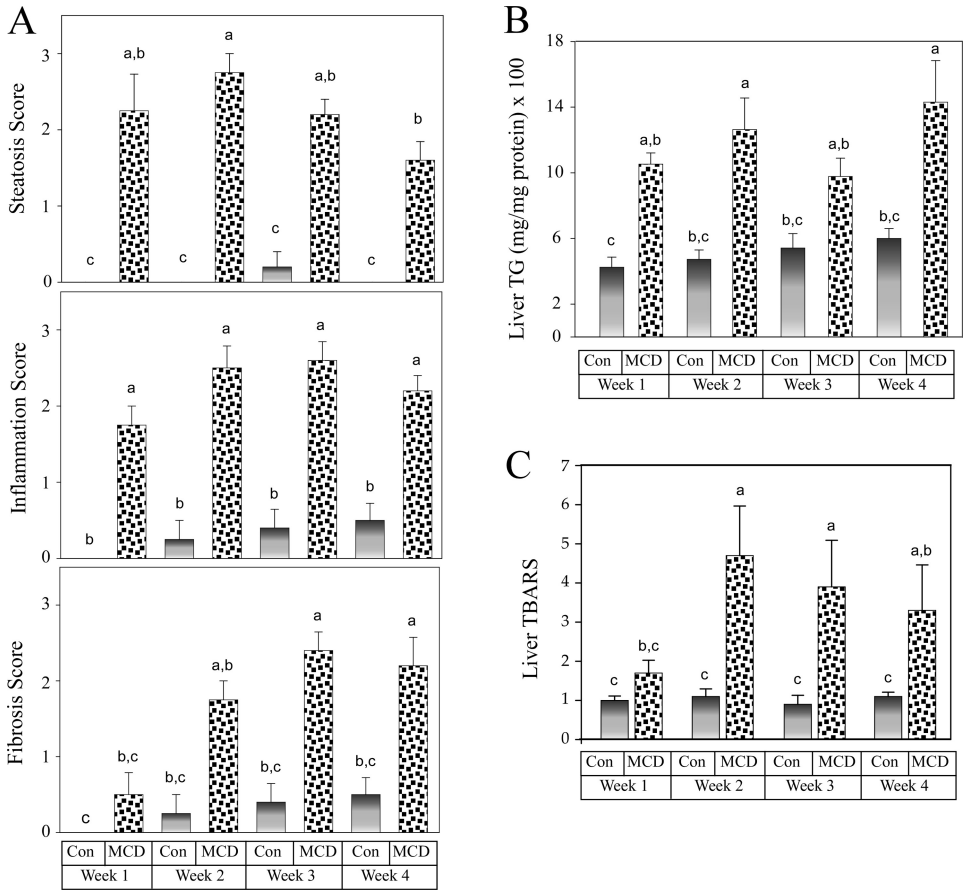

FIGURE 1. **MCD diet-induced steatohepatitis.** Male C57BL/6 mice were placed on control ($n = 4–5$) or MCD diets ($n = 4–5$) for 4 weeks. Paraffin-embedded sections were stained with hematoxylin and eosin and Masson's trichrome, examined in a blinded fashion by a board-certified pathologist, and graded for steatosis, inflammation, and fibrosis as described under "Materials and Methods." *A*, quantitation of steatosis, inflammation, and fibrosis is shown as means ± S.E. (*error bars*). The score for steatosis was zero in the control group (*Con*). Quantitation of hepatic triglyceride content (*B*) and oxidative stress (*C*) (TBARS) is shown as the means ± S.E. Data were analyzed by analysis of variance, and pairwise comparisons were made using Tukey's test. *Different letters* indicate significantly different values at $p < 0.05$.

levels were significantly elevated over the 4-week time course in mice fed the MCD diet with maximal serum ALT levels detected at 3 weeks (Table 1). A significant decrease in blood glucose levels was detected in mice fed the MCD diet (Table 1), which is consistent with an increase in insulin sensitivity that has been observed in mice fed a MCD diet (22). Low circulating lipid and glucose levels in MCD mice would predict that mice fed the MCD diet would consume more food; however, MCD mice do not consume more food than mice fed a control diet (23).

Histological examination of livers from mice fed a MCD diet showed marked steatosis over the 4-week time course (Fig. 1*A* and supplemental Fig. 1). Consistent with this observation, liver TG levels were significantly elevated in MCD diet-fed mice (Fig. 1*B*). Minimal inflammation and fibrosis were observed by histological examination during the first week, whereas mild to moderate inflammation and portal to periportal fibrosis were observed in the livers from mice fed a MCD diet thereafter (Fig. 1*A* and supplemental Fig. 1). In MCD-fed mice, liver oxidative stress, as measured by detecting TBARS, was not detected until after the mice had been on the experimental diet for 2 weeks (Fig. 1*C*).

PKC Isoform Activation—Membrane translocation is essential for PKC isoform activation (2, 24–27). PKC isoform activation can be assessed by determining the change in membrane and cytosol PKC protein content, an increase in PKC in the membrane and a reduction in PKC in the cytosol being indicative of activation. Liver-specific PKC isoform (ϵ and δ) activation was investigated in mice fed an MCD diet over the 4-week time course by determining membrane and cytosolic PKC protein content by immunoblotting. A classical PKC isoform (PKCα) was also assessed to evaluate specificity. There was a slight increase in membrane PKCα and PKCϵ protein (24 ± 4 and 43 ± 1%, respectively) detected in liver homogenates from mice fed an MCD diet for 1 week, suggesting that there was weak activation (Fig. 2, *A* and *B*, and Table 2). In contrast, there was a 436 ± 30% increase in membrane PKCδ under the same conditions. These results suggest that PKCδ is strongly activated by the MCD diet. There was a concomitant reduction in cytosolic PKCα and PKCϵ protein (−58 ± 14 and −48 ± 4%, respectively), whereas there was a surprising 162 ± 9% increase in cytosolic PKCδ protein. These results suggest that PKCδ protein levels are up-regulated in livers of mice fed the MCD diet for 1 week prior to the development of significant inflammation, oxidative stress parameters, and fibrosis. To verify the activation state of hepatic membrane PKCδ, we determined phosphorylation of PKCδ at Thr^{505} and Ser^{641}, two phosphorylation sites neces-

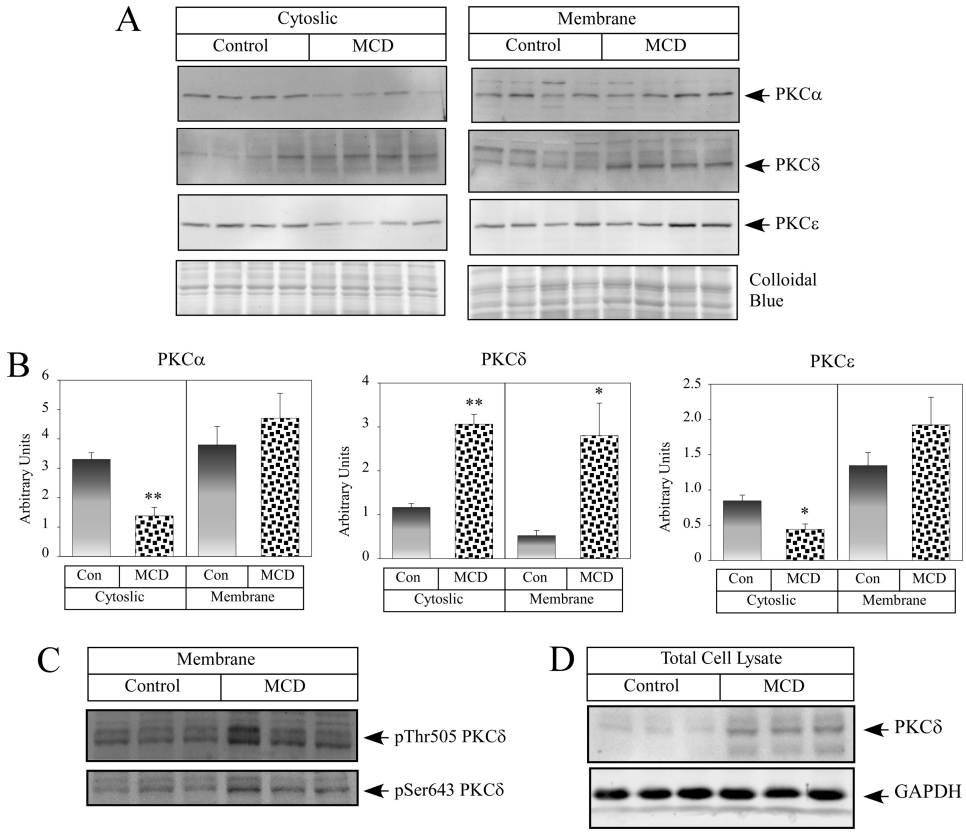

FIGURE 2. **MCD diet-induced hepatic PKCδ activation.** Liver tissue from four mice on control or MCD diets for 1 week was pulverized under liquid N_2 and fractionated into cytosolic and membrane protein or lysed in detergent-containing buffer. An equivalent amount of protein (50 μg) was analyzed by Western blotting. *A*, representative blots and images of the Colloidal Blue-stained gels are shown. *B*, quantitation of the immunoreactive bands minus background is shown as means ± S.E. (*error bars*) (*, $p < 0.05$; **, $p < 0.01$ *versus* control diet (*Con*)). *C*, PKCδ phosphorylation using antibodies to Thr^{505} and Ser^{643}. *D*, total cell lysate (25 μg of protein) from liver tissue was analyzed by immunoblotting for PKCδ and GAPDH expression.

TABLE 2
Percentage increase in MCD diet-induced hepatic PKC isoform protein levels

		Total cell lysate		Membrane		Cytosolic	
Isoform	Week	Increase	*p* value	Increase	*p* value	Increase	*p* value
PKCα	1			24 ± 4	0.423	−58 ± 14	0.002
PKCε	1			43 ± 1	0.230	−48 ± 4	0.011
PKCδ	1	264 ± 7	>0.001	436 ± 30	0.049	162 ± 9	0.001
PKCα	2			33 ± 3	0.394	−33 ± 3	0.295
PKCε	2			51 ± 1	0.322	−49 ± 2	0.012
PKCδ	2	145 ± 20	0.029	291 ± 3	0.001	21 ± 3	0.301
PKCα	3			−9 ± 3	0.768	−4 ± 8	0.904
PKCε	3			−15 ± 2	0.601	−62 ± 5	0.008
PKCδ	3	170 ± 6	0.001	272 ± 10	0.002	125 ± 13	0.025
PKCα	4			26 ± 2	0.196	29 ± 1	0.178
PKCε	4			−24 ± 2	0.104	6 ± 2	0.823
PKCδ	4	156 ± 12	0.004	512 ± 22	0.009	98 ± 10	0.006

sary for full activation (28). As shown in Fig. 2*C*, the MCD diet did indeed induce phosphorylation of PKCδ at Thr^{505} and Ser^{641}. To verify that PKCδ protein levels were up-regulated, total cell lysates were analyzed for PKCδ protein content. An increase of 264 ± 7% in hepatic PKCδ protein was observed in mice fed the MCD diet for 1 week (Fig. 2*D*).

Analysis of PKCδ protein content in the cytosolic and membrane fractions from mice fed the MCD diet for 2, 3, and 4 weeks revealed that PKCδ cytosolic protein content was significantly elevated (125 ± 13 and 98 ± 10%) by 3 and 4 weeks, respectively. A large increase in PKCδ membrane protein content (291 ± 3, 272 ± 10, and 512 ± 22%) was observed at 2, 3, and 4 weeks, respectively (Table 2 and supplemental Fig. 2, *A–C*). Elevated membrane phosphorylation of PKCδ at Thr^{505} and Ser^{641} (supplemental Fig. 3) was observed, and elevated PKCδ protein content in total cell lysates was observed over this same time course (supplemental Fig. 4).

In mice fed the MCD diet for 2, 3, or 4 weeks, cytosolic PKCε protein was significantly reduced only after 2 and 3 weeks of feeding (−49 ± 2 and −62 ± 5%, respectively) (Table 2 and supplemental Fig. 2, *A* and *B*). In contrast, no significant differences were observed in cytosolic PKCα protein in mice fed the MCD diet for 2, 3, and 4 weeks. Further, no significant differences were observed in PKCα and PKCε protein content in the membrane fraction (Table 2 and supplemental Fig. 2, *A–C*).

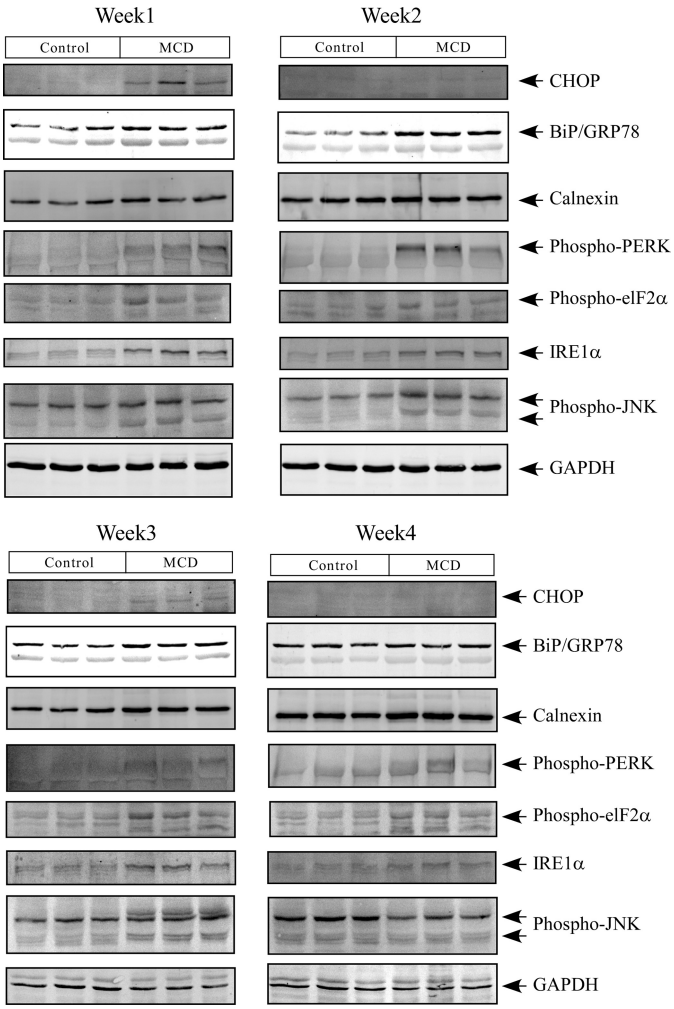

FIGURE 3. **MCD diet-induced hepatic ER stress activation.** Liver tissue from three mice on control or MCD diets for 1–4 weeks was lysed in detergent-containing buffer. The following antibodies were used for immunoblotting: phospho-JNK, phospho-PERK, phospho-eIF2α, calnexin, CHOP, BiP/GRP78, IRE1α, and GAPDH. Shown are representative blots.

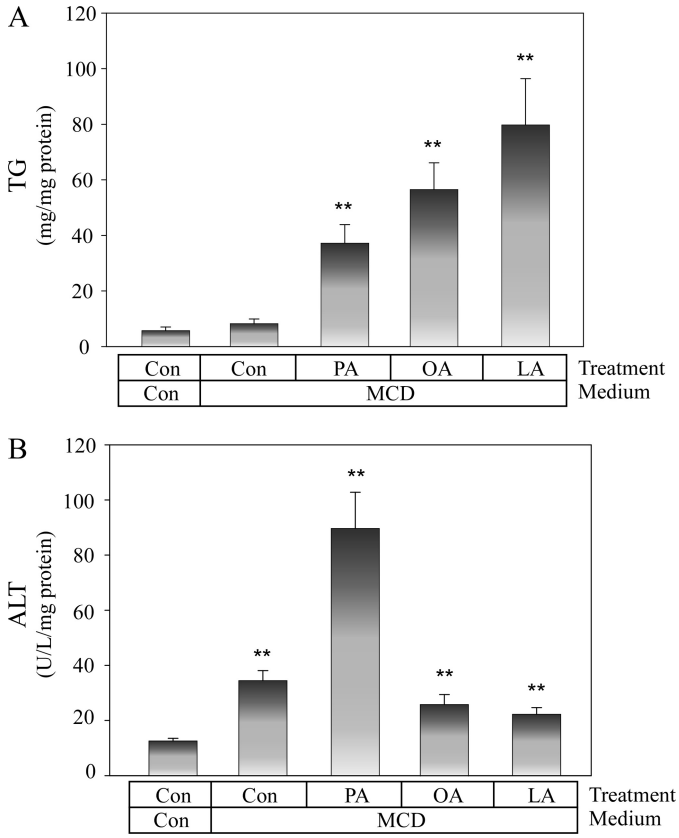

FIGURE 4. **Triglyceride accumulation and ALT release in McA cells.** McA cells were treated with control or MCD medium with palmitic (*PA*), oleic (*OA*), or linoleic (*LA*) acid or BSA (*Con*) for 16 h. Cells were homogenized and extracted to determine TG levels (*A*), or conditioned medium was concentrated to determine ALT levels (*B*). Quantitation of TG and ALT levels is shown as the means ± S.E. (*error bars*) (**, $p < 0.01$ *versus* non-treated control).

Hepatic ER Stress Activation—ER stress activation has been shown to be associated with high fat diets, lipid infusions, and MCD diet-induced steatosis (29–33). To gain insight into the time course of MCD diet-induced ER stress activation, ER stress markers were measured in mice fed an MCD diet over a 4-week time course. GAPDH protein expression remained constant throughout the 4 weeks of MCD feeding and was used as a loading control. As shown in Fig. 3, after 1 week on the MCD diet, PERK, eIF2α, and JNK phosphorylation were increased. Consistent with this result, CHOP, IRE1α, and BiP/GRP78 protein levels were also elevated. In contrast, calnexin was unaltered. IRE1α and BiP/GRP78 expression and PERK, eIF2α, and JNK phosphorylation remained elevated, whereas calnexin protein levels were increased in livers derived from mice fed the MCD diet for 2 and 3 weeks. CHOP induction was detected in week 3. Calnexin and IRE1α protein levels and PERK and eIF2α phosphorylation remained elevated at week 4, whereas CHOP and BiP/GRP78 protein levels were unaltered, and no change in JNK phosphorylation was detected.

TG Accumulation and ALT Induction in McA Cells—McA cells have been used as a model of steatosis (29, 34), and it has been demonstrated that short term culture of hepatic derived cells in MCD medium with serum results in steatosis and release of ALT (35, 36). McA cells were incubated for 16 h in serum-free BSA-containing medium (control) or MCD medium without or with palmitic, oleic, or linoleic acid complexed to BSA. There was a 6-, 10-, and 14-fold increase in cellular TG accumulation in cells incubated with palmitic, oleic, and linoleic acids, respectively, in MCD medium compared with control medium (Fig. 4*A*), indicating that free fatty acid treatment is necessary to induce lipid accumulation in McA cells cultured in serum-free medium. The MCD medium also resulted in a 3-fold increase in ALT release, whereas incubations in MCD medium containing palmitic acid demonstrated a 7-fold increase in ALT release (Fig. 4*B*). These results indicate that palmitic acid strongly enhances MCD medium-mediated McA cell dysfunction.

PKCδ Activation in McA Cells—We next determined the protein content and phosphorylation state of PKCδ in membrane and cytosolic fractions from McA cells treated with MCD medium without or with fatty acids incubated for 1, 8, and 16 h. There was an increase in PKCδ membrane protein content (Fig. 5, *A* and *B*) concomitant with a reduction in PKCδ cytosolic protein content (Fig. 5, *A* and *B*) in cells treated at all three time points in MCD medium with fatty acids. Maximal PKCδ phosphorylation (>2-fold increase

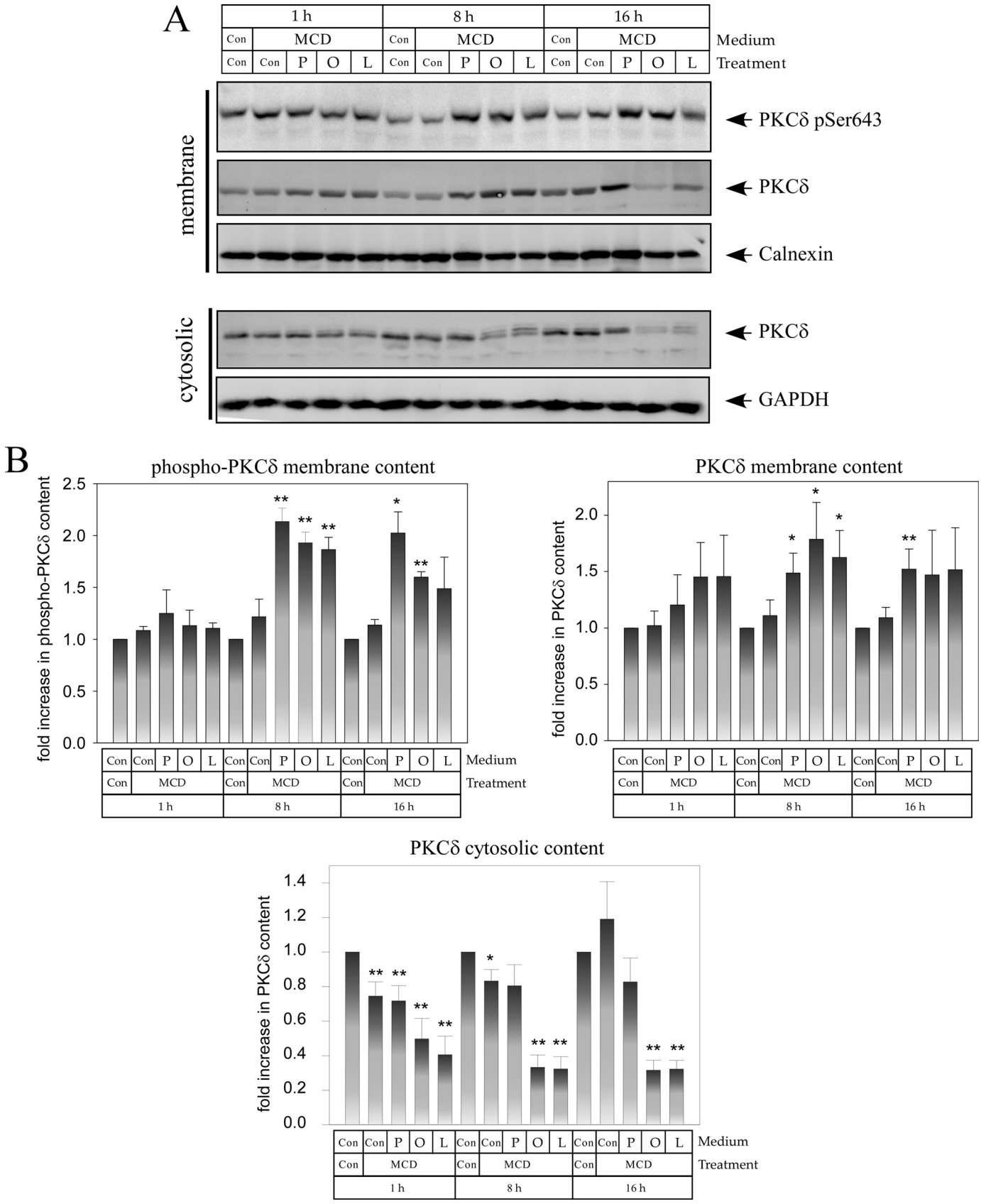

FIGURE 5. **Time course of PKCδ activation in McA cells.** McA cells were treated as described in Fig. 4 for 1 h, 8 h, or 16 h. Fatty acid treatments were palmitic (*P*), oleic (*O*), or linoleic (*L*) acids. Cells were homogenized and fractionated to generate membrane and cytosolic fractions. PKCδ, phospho-PKCδ (pSer643), calnexin, and GAPDH were assessed by immunoblotting. *A*, shown are representative blots from at least three independent experiments. *B*, quantitation of the immunoreactive bands minus background for PKCδ and phospho-PKCδ membrane content, and PKCδ cytosolic content are shown as the means ± S.E. (*, $p < 0.05$; and **, $p < 0.01$ *versus* non-treated control).

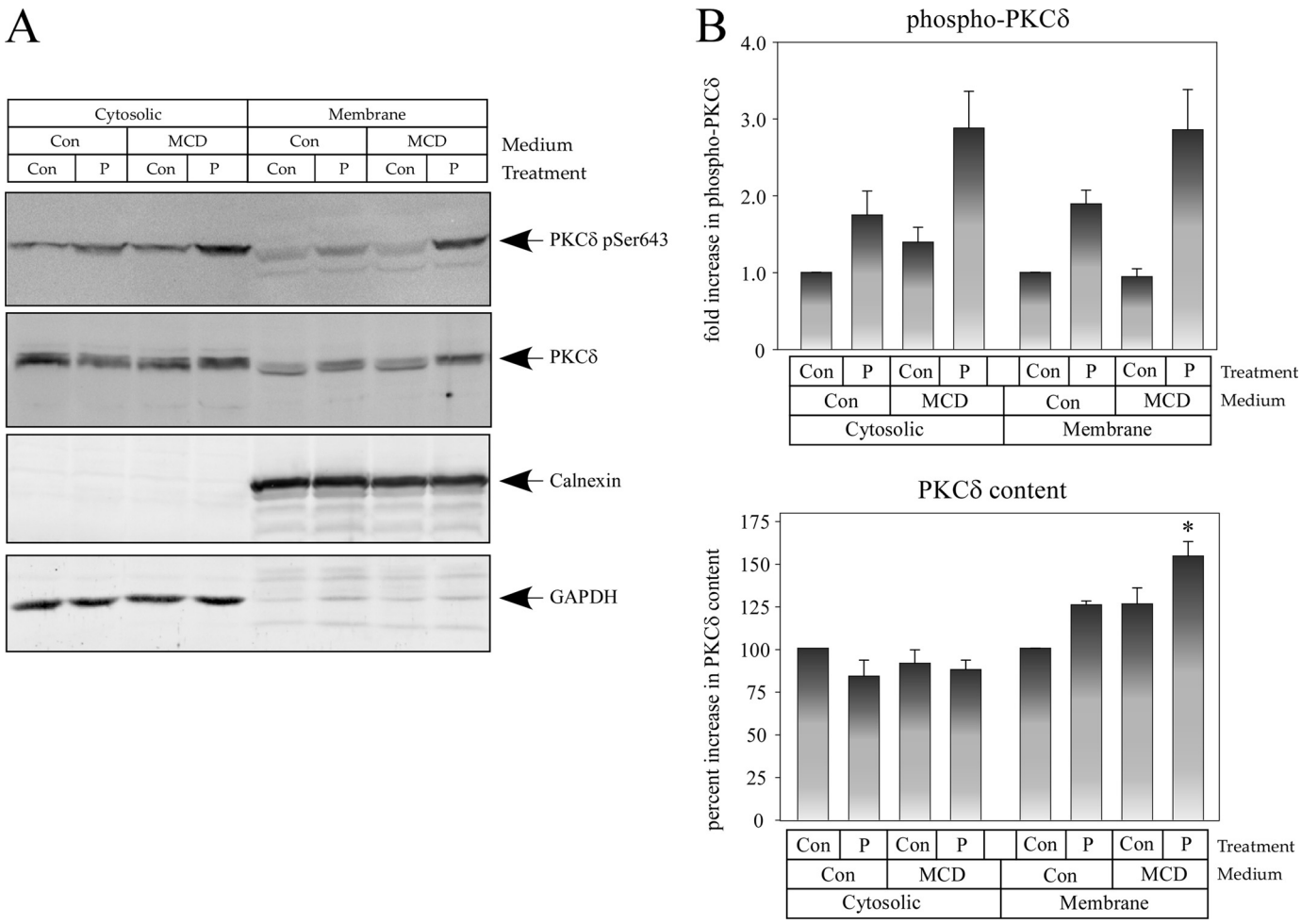

FIGURE 6. **MCD medium-induced PKCδ activation in McA cells.** McA cells were treated with palmitic acid (*P*) in control (*Con*) or MCD medium for 8 h and processed as described in the legend to Fig. 5. *A*, representative blots from at least three independent experiments. *B*, quantitations of the immunoreactive bands minus background for PKCδ and phospho-PKCδ are shown as the means ± S.E. (*error bars*) (*, $p < 0.05$ *versus* palmitic acid-treated control).

compared with control non-treated cells) was observed in the membranes from cells treated for 8 and 16 h in MCD medium with added palmitic acid. Significant increases in PKCδ phosphorylation were also observed in cells treated for 8 and 16 h in MCD medium with added oleic and linoleic acids (Fig. 5*B*).

To assess whether palmitic acid activates PKCδ in the absence of MCD medium and to confirm the effect of palmitic acid on PKCδ activation in the presence of MCD medium, we determined the phosphorylation state and protein content of PKCδ in membrane and cytosolic fractions from McA cells treated with control or MCD medium without or with palmitic acid incubated for 8 h. MCD medium enhanced palmitic acid-stimulated membrane PKCδ phosphorylation (2.8 ± 0.5-fold increase *versus* a 1.9 ± 0.2-fold increase compared with control non-treated cells) and to a lesser degree PKCδ membrane content (Fig. 6). Surprisingly, MCD medium stimulated cytosolic PKCδ phosphorylation (>2.8-fold increase compared with control non-treated cells). Taken together, the results presented in Figs. 5 and 6 indicate that MCD medium with added fatty acids, and in particular palmitic acid, activates PKCδ *in vitro*, which is consistent with our observation that an MCD diet activates hepatic PKCδ *in vivo*.

ER Stress Activation in McA Cells—ER stress activation was determined in cells incubated for 1, 8, and 16 h in control medium or MCD medium without or with added fatty acids (Fig. 7*A*). In cells incubated for 1 h, we were unable to detect CHOP induction or any changes to BiP/GRP78 or GAPDH protein levels in any of the treatments. JNK activation was observed in cells treated with MCD medium with fatty acids; however, only in palmitic acid-treated cells was JNK activation significantly elevated (183 ± 74%). eIF2α phosphorylation was also elevated in cells treated with palmitic acid (153 ± 42%), consistent with JNK activation. In cells incubated for 8 h, no changes were observed in BiP/GRP78 and GAPDH protein levels in any of the treatments. In contrast, there was a 2.8–3.9-fold increase in CHOP in the MCD medium irrespective of fatty acid addition. Maximal CHOP induction (391 ± 118%) and significantly elevated PERK, eIF2α, and JNK phosphorylation (195 ± 22, 201 ± 28, and 716 ± 269%, respectively) were detected in cells treated with palmitic acid. Sustained PERK and JNK phosphorylation (526 ± 83 and 167 ± 39%, respectively) and CHOP induction (882 ± 362%) were observed in cells treated for 16 h with palmitic acid in MCD medium compared with control cells. Similar results with palmitic acid in MCD medium on PERK and JNK

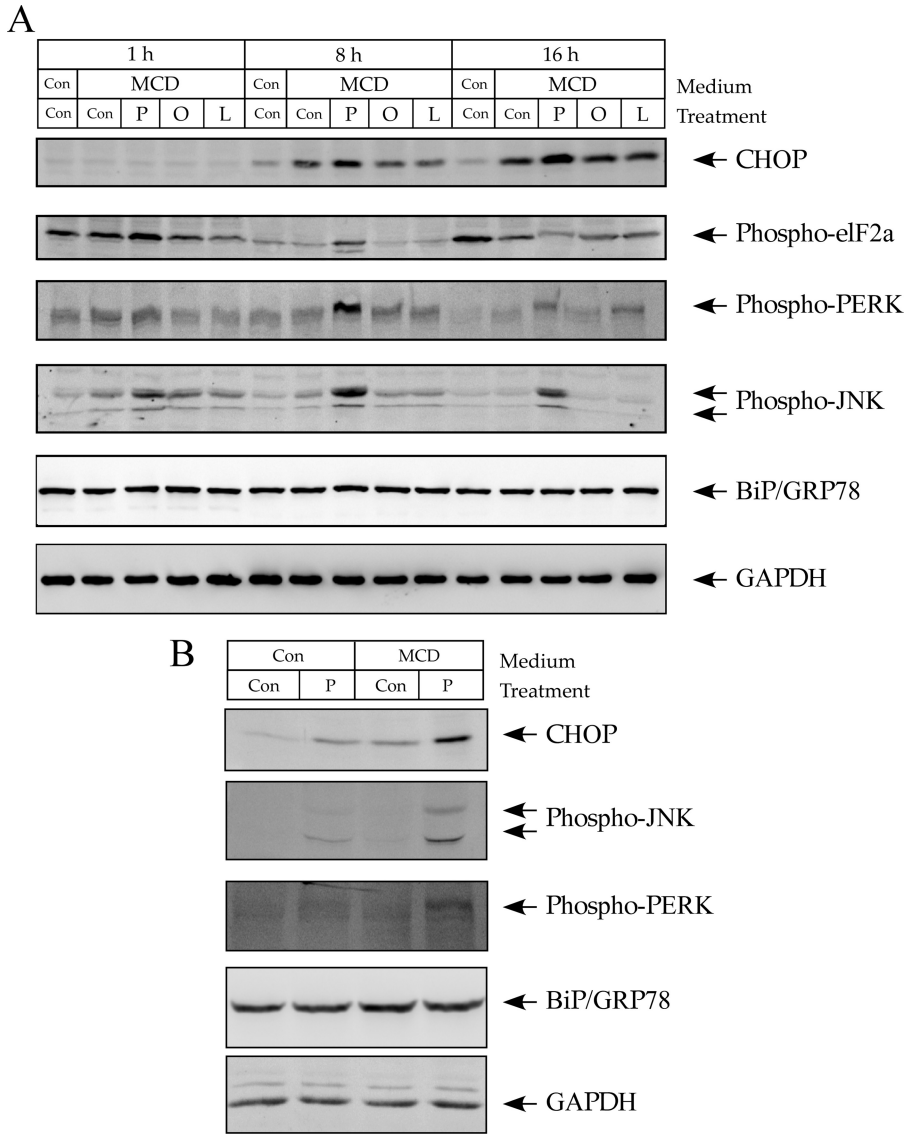

FIGURE 7. **MCD medium-induced ER stress activation in McA cells.** Total cell lysate (70 μg of protein) was analyzed by immunoblotting for phospho-JNK, phospho-PERK, phospho-eIF2α, CHOP, BiP/GRP78, and GAPDH. *A*, McA cells were treated as described in Fig. 4 for 1, 8, or 16 h. *P*, palmitic acid; *O*, oleic acid; *L*, linoleic acid; *Con*, control. *B*, McA cells were treated as described in the legend to Fig. 6 for 16 h. Shown are representative blots from three independent experiments.

phosphorylation were observed in primary mouse hepatocytes (data not shown).

To assess whether palmitic acid activates ER stress in the absence of MCD medium and confirm the effect of palmitic acid on ER stress activation in the presence of MCD medium, McA cells were incubated for 16 h without or with palmitic acid in control or MCD medium. As shown in Fig. 7*B*, no changes were observed in BiP/GRP78 and GAPDH protein levels in any of the treatments. In contrast, a 3.5 ± 0.8- and 3.4 ± 0.6-fold increase in JNK activation and CHOP induction, respectively was detected in palmitic acid-treated cells in control medium, whereas in palmitic acid-treated cells in MCD medium, a 11.5 ± 3.0- and 15.7 ± 2.5-fold increase in JNK activation and CHOP induction, respectively, was detected, indicating that MCD medium enhances palmitic acid-stimulated ER stress. Consistent with this conclusion, a 6.9 ± 3.1-fold increase in PERK activation was detected in cells incubated with palmitic acid in MCD medium compared with control medium. The results presented in Fig. 7 indicate that MCD medium with palmitic acid activates ER stress, which is consistent with our observation that MCD diet activates hepatic ER stress *in vivo*.

Chemical Chaperone Inhibition of ER Stress and PKCδ in McA Cells—We have previously reported that TMAO, a widely used naturally occurring osmolyte/chemical chaperone (37–40), blocks TNFα- and thapsigargin-induced ER stress and PKCδ activation (19). To assess whether TMAO blocks MCD medium with palmitic acid-induced ER stress activation, McA cells were preincubated for 6 h with various concentrations of TMAO in control or MCD medium prior to treatment for 16 h. As shown in Fig. 8*A*, no changes were observed in BiP/GRP78 and GAPDH protein levels in any of the treatments. In contrast, a dose-dependent reduction in JNK and PERK activation and CHOP induction were observed in

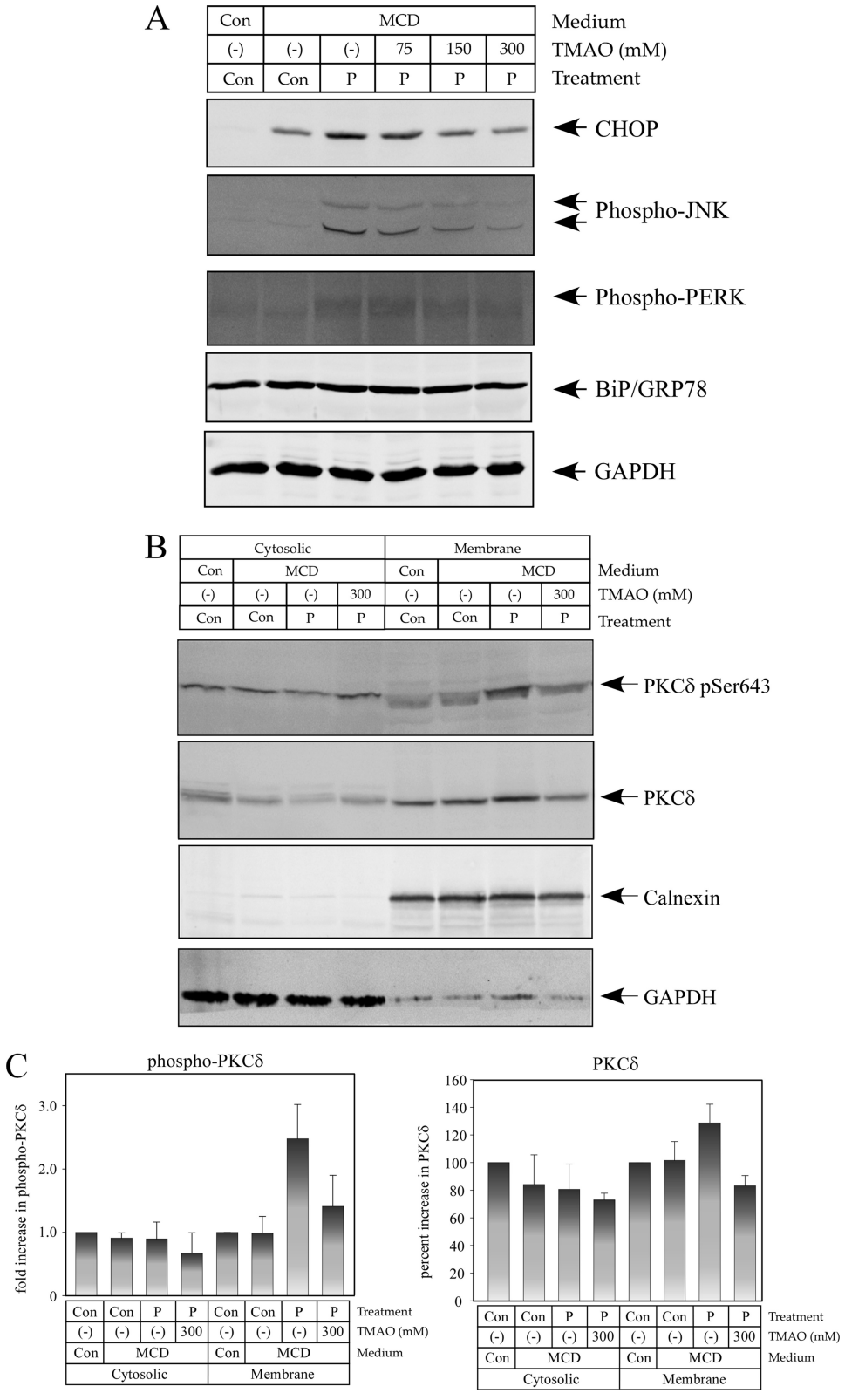

FIGURE 8. **Chemical chaperone inhibition of MCD medium-induced ER stress and PKCδ activation in McA cells.** McA cells were pretreated with TMAO as indicated for 6 h and then treated with control or MCD medium with palmitic acid (*P*) or BSA (*Con*) for 16 h. *A*, total cell lysate (70 μg of protein) was analyzed by immunoblotting for ER stress markers as shown in Fig. 7. *B*, cells were homogenized and fractionated to generate membrane and cytosolic fractions. PKCδ, phospho-PKCδ (*pSer643*), calnexin, and GAPDH were assessed by immunoblotting. *C*, quantitation of the immunoreactive bands minus background for PKCδ and phospho-PKCδ membrane content and PKCδ cytosolic content are shown as the means ± S.E. (*error bars*).

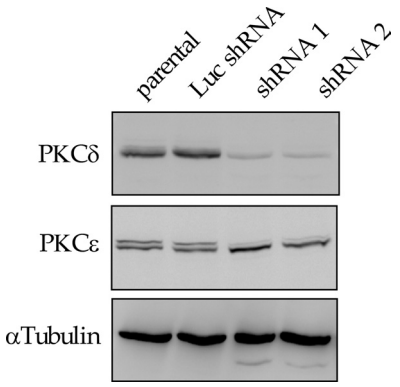

FIGURE 9. **Knockdown of PKCδ in McA cells.** 29-mer shRNAs were designed and cloned into pLKO.1, and viral particles were generated as described under "Materials and Methods." Total cell lysate from McA cells stably expressing PKCδ shRNA 1 or 2 or a Luc shRNA was analyzed for protein expression 7 days after puromycin selection. Total cell lysate (30 μg of protein) was analyzed by immunoblotting for PKCδ, PKCε, and α-tubulin. Representative blots from three independent experiments are shown.

cells pretreated with TMAO. Further, pretreatment of cells with TMAO reduced MCD medium with palmitic acid stimulated membrane PKCδ phosphorylation by 43 ± 20% and membrane PKCδ protein content by 36 ± 6% (Fig. 8, *B* and *C*). These results indicate that ER stress plays a role in PKCδ activation in cells treated with MCD medium with palmitic acid.

TG Accumulation and ALT Induction in PKCδ-deficient McA Cells—We next determined the role of PKCδ in TG accumulation and ALT release. McA cells stably expressing 29-mer PKCδ shRNAs (20) or a luciferase (Luc) control shRNA (41) were generated as described under "Materials and Methods." Two shRNAs targeting unique sites in the PKCδ mRNA were used to exclude potential off-target effects. Cells expressing the PKCδ shRNAs or Luc control shRNA were treated without or with MCD medium with fatty acids for 16 h, and then TG accumulation and ALT were measured. PKCδ protein levels were reduced by >80% compared with cells expressing the Luc control shRNA (Luc control cells) (Figs. 9 and 11). No differences in PKCε or α-tubulin were observed in cells expressing the PKCδ shRNA (Fig. 9). TG accumulation was reduced in cells expressing PKCδ shRNA 1 compared with cells expressing PKCδ shRNA 2 or the Luc control shRNA, except with oleic acid incubation. No difference was observed in TG accumulation between cells expressing PKCδ shRNA 2 and the Luc control shRNA (Fig. 10*A*). In contrast, ALT release induced by MCD medium with fatty acids was completely blocked in cells expressing both PKCδ shRNAs (Fig. 10*B*). These results indicate that PKCδ is necessary for McA cell dysfunction.

ER Stress Activation and Cell Death in PKCδ-deficient McA Cells—The requirement for PKCδ in ER stress activation was evaluated in PKCδ knockdown and control cells incubated for 8 h in control or MCD medium without or with added fatty acids. Maximal CHOP induction and significantly elevated PERK and JNK phosphorylation were detected in control Luc shRNA cells treated with palmitic acid in MCD medium. Interestingly, CHOP induction and PERK and JNK phosphorylation were completely blocked in cells expressing the PKCδ

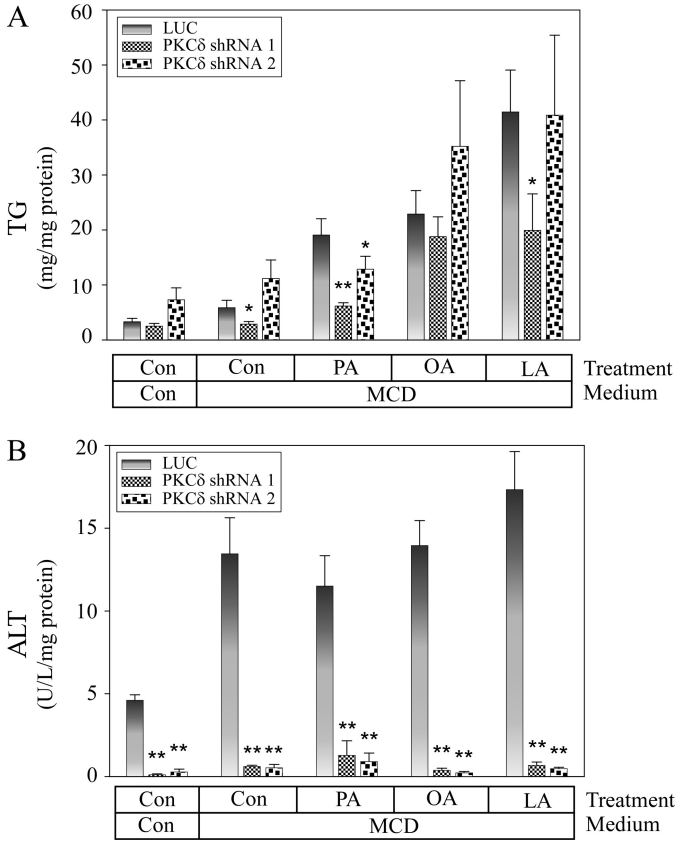

FIGURE 10. **Role of PKCδ in TG accumulation and ALT release in McA cells.** McA cells expressing PKCδ shRNAs or a Luc control were treated as described in the legend to Fig. 4. *PA*, palmitic acid; *OA*, oleic acid; *LA*, linoleic acid. Quantitations of TG (*A*) and ALT (*B*) levels are shown as the means ± S.E. (*error bars*) (*, $p < 0.05$; **, $p < 0.01$ *versus* non-treated control).

shRNAs (Fig. 11). No changes were observed in α-tubulin protein levels in cells expressing the PKCδ shRNAs. These results indicate that knockdown of PKCδ prevented ER stress.

To assess whether the effect of PKCδ knockdown relates to cell survival, PKCδ knockdown and control cells were incubated for 24 h in control or MCD medium without or with palmitic acid. There was a significant increase in cell viability in the PKCδ knockdown cell lines treated with palmitic acid in the absence or presence of MCD medium (Fig. 12*A*). Next, DNA content was used to assess cell number in PKCδ knockdown and control cells. In MCD medium, palmitic acid significantly reduced total DNA in control cells but not in cells expressing the PKCδ shRNAs (Fig. 12*B*). Palmitic acid addition also stimulated an increase in apoptotic nuclei in control (Luc shRNA) cells but not in cells expressing the PKCδ shRNA 2 (Fig. 12*C*).

The role of ER stress in MCD medium with palmitic acid-induced cell death was tested in cells pretreated with TMAO. As shown in Fig. 12*D*, a 3.9-fold increase was observed in the uptake of PI, a vital nucleic acid-staining dye that penetrates cells with a compromised plasma membrane. In cells pretreated with TMAO, a significant reduction in PI uptake was observed, indicating that ER stress contributes to MCD medium with palmitic acid-induced cell death.

Finally, the specificity of the PKCδ knockdown effect on palmitic acid-induced cell death was evaluated using a mu-

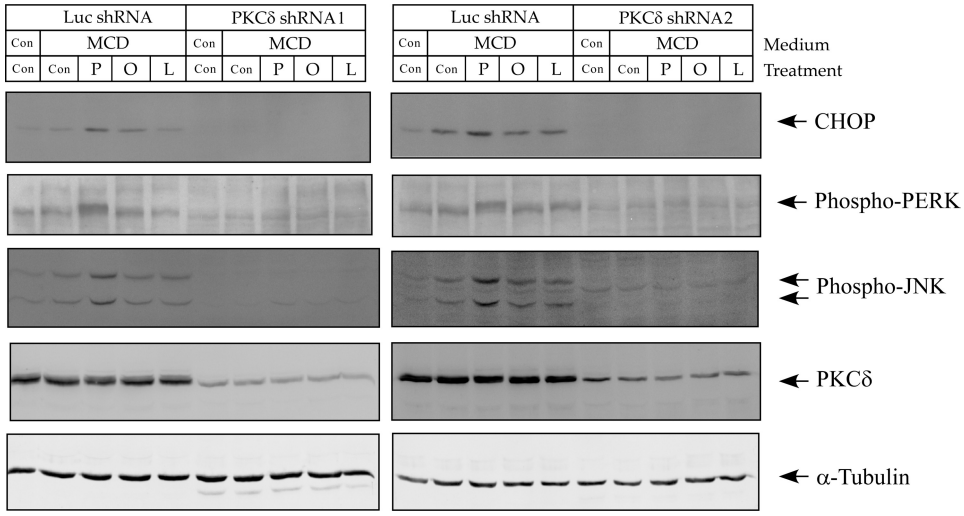

FIGURE 11. **Role of PKCδ in MCD medium-induced ER stress activation in McA cells.** McA cells expressing PKCδ shRNAs or a Luc control were treated for 8 h as described in the legend to Fig. 5. *P*, palmitic acid; *O*, oleic acid; *L*, linoleic acid. Total cell lysate (70 μg of protein) was analyzed by immunoblotting for phospho-JNK, phospho-PERK, CHOP, and α-tubulin. Shown are representative blots from three independent experiments.

tated shRNA hybridization site mouse PKCδ (supplemental Fig. 5). Cell death was assessed by determining the uptake of PI. As shown in Fig. 13*A*, a significant reduction in cell death was detected in PKCδ knockdown cells treated with palmitic acid. Wild type mouse PKCδ (mPKCδ) did not rescue the effect of palmitic acid in the PKCδ knockdown cells. In contrast, the mutant mPKCδ, which was resistant to the PKCδ shRNA (Fig. 13*B*), rescued the effect of palmitic acid on cell death in PKCδ knockdown cells. Taken together, the results presented in Figs. 12 and 13 indicate that PKCδ regulates palmitic acid-induced lipotoxicity.

DISCUSSION

The histological features of NASH in humans are similar to those in rodents fed a diet deficient in methonine and choline. In the MCD model, hepatic steatosis results primarily from an increase in free fatty acid uptake coupled with decreased TG export, which leads to inflammation, oxidative damage, and hepatocyte cell death, recapitulating the progression from steatosis to steatohepatitis observed in humans (42–44). We determined the activation of two novel PKC isoforms (PKCδ and PKCϵ) and a classical PKC isoform (PKCα) during the development of steatohepatitis in mice fed the MCD diet. Because translocation from the cytosol to membranes and/or organelles is necessary for PKC activation, we determined whether the hepatic PKC content in the membrane and cytosolic fraction was altered by the MCD diet. Only PKCδ protein content was significantly increased in the membrane fraction over the 4-week time course of the diet. Surprisingly, PKCδ protein content was also significantly increased in the cytosolic fraction and total cell lysate over the same time course. Although total PKCδ protein levels were increased from 3.7- to 6.1-fold, the increase in PKCδ in the membrane fraction was proportionally greater (146–356%). In addition, we observed that phosphorylation of Ser^{643} and Thr^{505} in membrane-associated PKCδ was strongly induced in the MCD-fed mice. Taken together, these data indicate that the MCD diet stimulates both PKCδ expression and activation. In contrast to our findings, PKCϵ activation rather than PKCδ activation has been shown to play a role in steatosis and liver dysfunction induced by a diet high in unsaturated fat (7, 45). However, a recent study suggests that saturated fatty acids mediate hepatocyte injury in mice fed an MCD diet (43). The changes observed in hepatic PKCδ activation and protein content after 1 week on the MCD diet were coincident with steatosis, mild inflammation, and liver dysfunction (serum ALT elevation). Significant inflammation, oxidative stress, and fibrosis, markers of advanced liver damage, were detected in mice fed the MCD diet for 2 weeks. Thus, these data indicate that PKCδ activation and elevated protein content are associated with steatosis and mild inflammation that occurs prior to the development of steatohepatitis observed in the MCD diet model. Interestingly, elevated PKCδ expression and activation were consistently observed during the progression to steatohepatitis.

ER stress activation in the MCD diet model of steatohepatitis has previously been shown to be present after either 2 (15), 3 (32), or 4 weeks (33) of feeding. In the present study, we observed that ER stress activation occurred throughout the progression of steatosis to steatohepatitis. Our results show that there is an increase in CHOP, IRE1α, and BiP/GRP78 protein levels and PERK, eIF2α, and JNK phosphorylation in the liver of mice fed the MCD diet. This result is consistent with previous studies showing that the unfolded protein response can be detected in the liver (and adipose tissue) from obese ob/ob and high fat diet-fed mice (30, 31), animal models that develop fatty livers but do not develop NASH. Further, overexpression of the chaperone Bip/GRP78 in the liver reduces ER stress markers and attenuates steatosis in obese ob/ob mice (46).

Cells incubated with MCD medium in the presence of serum, a lipid source, store TG and exhibit hepatocyte dysfunction (35, 36). It is unclear if saturated or unsaturated fatty acids contributed to the dysfunction observed. We found that fatty acids were necessary for TG storage in MCD medium-treated cells, although MCD medium alone was sufficient to

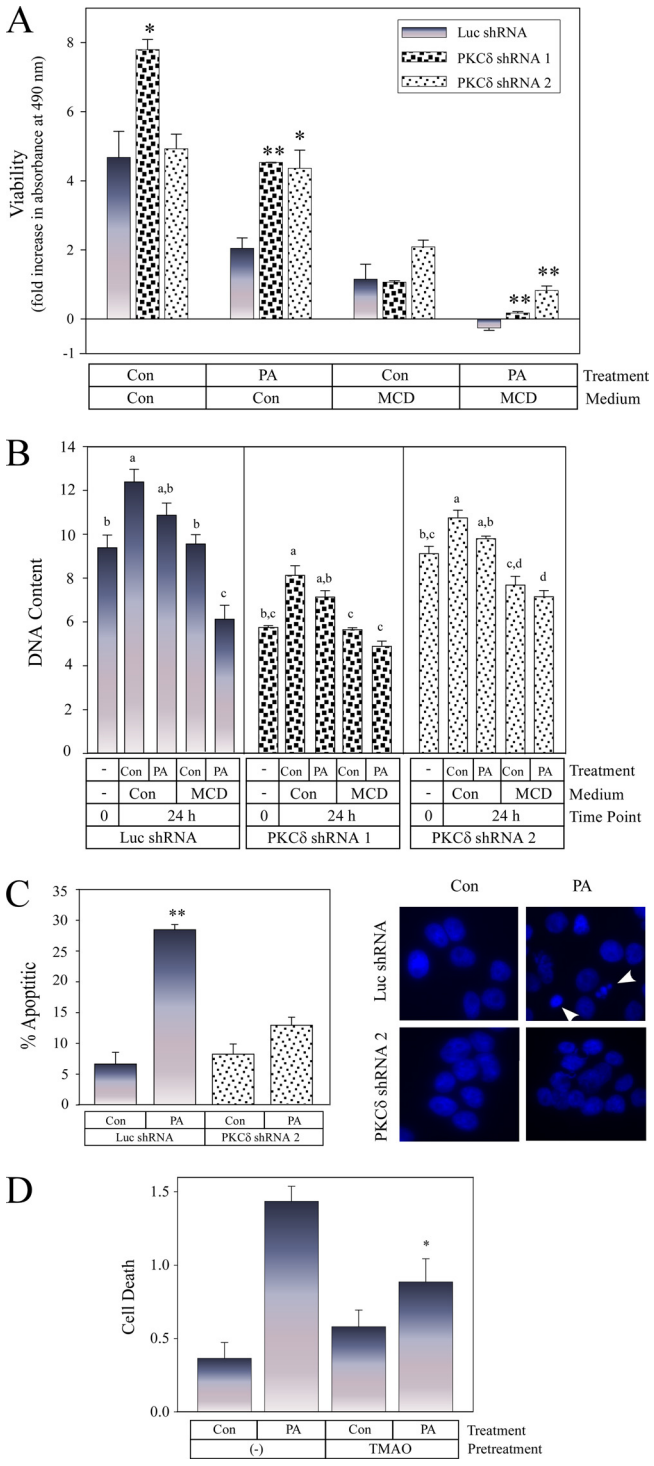

FIGURE 12. **Role of PKCδ and ER stress in MCD medium/palmitic acid-induced cell death in McA cells.** McA cells expressing PKCδ shRNAs or a Luc control were treated with control or MCD medium with palmitic acid (*PA*) or BSA (*Con*) for 24 h. *A*, cell viability was determined using the MTS assay (*, $p < 0.05$; **, $p < 0.01$ *versus* Luc control). *B*, DNA content was determined using the CyQuant assay. Data were analyzed by analysis of variance, and pairwise comparisons were made using Tukey's test. *Different letters* indicate significantly different values at $p < 0.05$. *C*, apoptosis was determined by counting the number of apoptotic nuclei in fixed cells stained with DAPI. Shown are quantitations of three independent experiments, as the means ± S.E. (*error bars*) (**, $p < 0.01$ *versus* control-treated) and representative images. *D*, cell death was assessed by determining PI uptake as described under "Materials and Methods." Cells were pretreated with 300 mM TMAO for 4 h. Shown are quantitations of four independent experiments, as the means ± S.E. (*, $p < 0.05$ *versus* PA-treated).

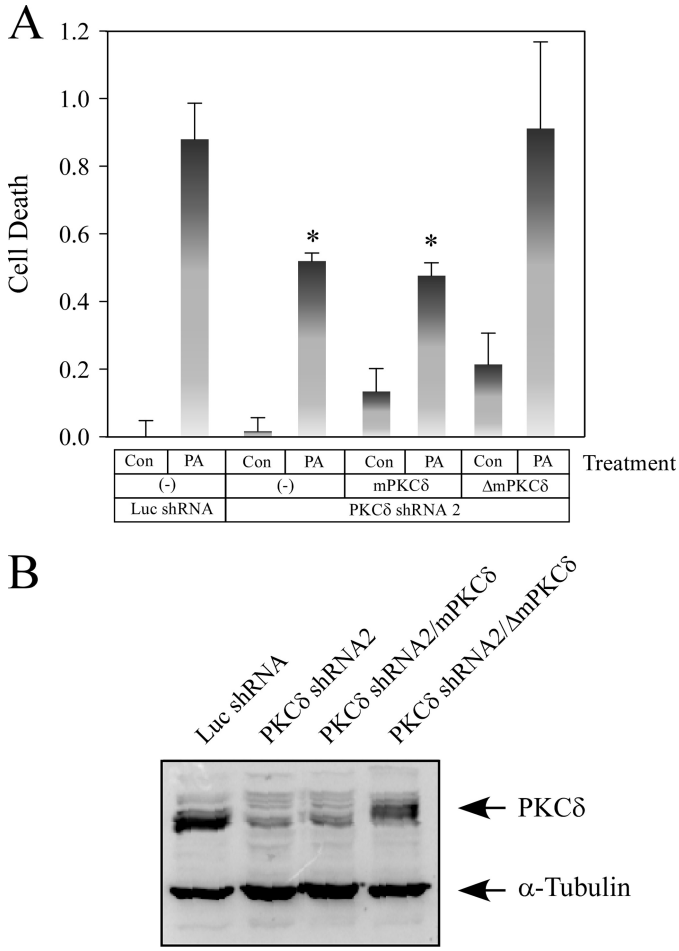

FIGURE 13. **shRNA rescue of PKCδ in MCD medium/palmitic acid-induced cell death in McA cells.** *A*, McA cells stably expressing Luc shRNA or PKCδ shRNA 2 or co-expressing PKCδ shRNA 2 and mPKCδ or a mutant mPKCδ (Δ*mPKCδ*) were generated as described under "Materials and Methods." *A*, total cell lysate (30 μg of protein) was analyzed by immunoblotting for PKCδ and α-tubulin. *B*, cells were treated with control or MCD medium with palmitic acid (*PA*) or BSA (*Con*) for 24 h, and cell death was assessed by determining PI uptake as described under "Materials and Methods." Shown are quantitations of three independent experiments as the means ± S.E. (*, $p < 0.05$ *versus* control-treated).

induce ALT release and CHOP protein induction. These results suggest that a deficiency in methonine and choline directly affects hepatocyte function. In the present study, we were unable to detect ER stress activation by oleic or linoleic acids in MCD medium above that observed in MCD medium alone. ER stress activation by oleic acid has not been consistently detected (29, 47, 48). In contrast, MCD medium in the presence of palmitic acid was able to induce the greatest amount of ALT release by parental McA cells. We also found that ER stress activation (JNK, PERK, and eIF2α phosphorylation and CHOP protein induction) was greatest in palmitic acid/MCD medium-treated cells. JNK, PERK, and eIF2α phosphorylation was also greatest in primary mouse hepatocytes treated with palmitic acid/MCD medium (data not shown). These results are in agreement with previous reports indicating that palmitic acid activates the IRE1 and PERK branches of the unfolded protein response, leading to sustained JNK activation, CHOP induction, and eventually cell death in hepatocytes (48–51). Our current results demon-

strate that reduced PKCδ protein levels in McA cells using RNAi blocked free fatty acid/MCD medium-mediated ER stress activation (JNK and PERK phosphorylation and CHOP protein induction). This observation extends our recent findings that a reduction in PKCδ protein content blunted thapsigargin-stimulated JNK activation and CHOP protein induction (19). Tunicamycin-stimulated JNK activation is also blunted in Neuro2a cells with reduced PKCδ protein expression (52). Taken together, these data indicate that PKCδ may play a role in the propagation of the ER stress signal.

Our results showing that MCD medium with palmitic acid induced sustained JNK activation and CHOP induction are consistent with previous reports showing that palmitic acid induces JNK activation and CHOP protein levels and stimulates cell death in hepatocytes (32, 53). Although CHOP is known to propagate ER stress-mediated cell death in cell and animal models (54, 55) and has been shown to play a role in cholestatis-induced hepatocyte cell injury and liver fibrosis (56), the role of CHOP in palmitic acid-induced hepatocyte cell death has recently been questioned (32). Our observation that JNK activation and CHOP induction are blocked in cells with reduced PKCδ protein levels suggests that PKCδ plays a role in hepatocyte cell death. Indeed, cell viability and cell number were significantly increased in PKCδ knockdown cells incubated in MCD medium with palmitic acid. Furthermore, a reduction in the number of apoptotic nuclei and the uptake of PI was observed in PKCδ knockdown cells, compared with control cells incubated in MCD medium plus palmitic acid. Finally, the specificity of the PKCδ knockdown on cell death was confirmed using shRNA rescue. Taken together, these data suggest that PKCδ plays a role not only in the propagation of the ER stress signal but also in cell death.

Acknowledgments—We thank Dr. Janet Sparks for critically reviewing the manuscript. We are grateful to Dr. Didier Trono for kindly providing the pRRE, pRev, and pMD2G plasmids and Robert Weinberg for kindly providing the pLKO.1 plasmid.

REFERENCES

1. Newton, A. C. (2010) *Am. J. Physiol. Endocrinol. Metab.* **298,** E395–E402
2. Giorgione, J. R., Lin, J. H., McCammon, J. A., and Newton, A. C. (2006) *J. Biol. Chem.* **281,** 1660–1669
3. Boden, G., She, P., Mozzoli, M., Cheung, P., Gumireddy, K., Reddy, P., Xiang, X., Luo, Z., and Ruderman, N. (2005) *Diabetes* **54,** 3458–3465
4. Griffin, M. E., Marcucci, M. J., Cline, G. W., Bell, K., Barucci, N., Lee, D., Goodyear, L. J., Kraegen, E. W., White, M. F., and Shulman, G. I. (1999) *Diabetes* **48,** 1270–1274
5. Itani, S. I., Ruderman, N. B., Schmieder, F., and Boden, G. (2002) *Diabetes* **51,** 2005–2011
6. Schmitz-Peiffer, C., Browne, C. L., Oakes, N. D., Watkinson, A., Chisholm, D. J., Kraegen, E. W., and Biden, T. J. (1997) *Diabetes* **46,** 169–178
7. Samuel, V. T., Liu, Z. X., Wang, A., Beddow, S. A., Geisler, J. G., Kahn, M., Zhang, X. M., Monia, B. P., Bhanot, S., and Shulman, G. I. (2007) *J. Clin. Invest.* **117,** 739–745
8. Deleted in proof
9. Frangioudakis, G., Burchfield, J. G., Narasimhan, S., Cooney, G. J., Leitges, M., Biden, T. J., and Schmitz-Peiffer, C. (2009) *Diabetologia* **52,** 2616–2620
10. Farrell, G. C., and Larter, C. Z. (2006) *Hepatology* **43,** Suppl. 1, S99–S112
11. Jou, J., Choi, S. S., and Diehl, A. M. (2008) *Semin. Liver Dis.* **28,** 370–379
12. Day, C. P., and James, O. F. (1998) *Gastroenterology* **114,** 842–845
13. Kirsch, R., Clarkson, V., Shephard, E. G., Marais, D. A., Jaffer, M. A., Woodburne, V. E., Kirsch, R. E., and Hall Pde, L. (2003) *J. Gastroenterol. Hepatol.* **18,** 1272–1282
14. Anstee, Q. M., and Goldin, R. D. (2006) *Int. J. Exp. Pathol.* **87,** 1–16
15. Henkel, A. S., Elias, M. S., and Green, R. M. (2009) *J. Biol. Chem.* **284,** 31807–31816
16. Svedberg, J., Björntorp, P., Smith, U., and Lönnroth, P. (1990) *Diabetes* **39,** 570–574
17. Shin, O. H., Mar, M. H., Albright, C. D., Citarella, M. T., da Costa, K. A., and Zeisel, S. H. (1997) *J. Cell. Biochem.* **64,** 196–208
18. Yen, C. L., Mar, M. H., Craciunescu, C. N., Edwards, L. J., and Zeisel, S. H. (2002) *J. Nutr.* **132,** 1840–1847
19. Greene, M. W., Ruhoff, M. S., Burrington, C. M., Garofalo, R. S., and Oreña, S. J. (2010) *Cell. Signal.* **22,** 274–284
20. Greene, M. W., Ruhoff, M. S., Roth, R. A., Kim, J. A., Quon, M. J., and Krause, J. A. (2006) *Biochem. Biophys. Res. Commun.* **349,** 976–986
21. Cullen, B. R. (2006) *Nat. Methods* **3,** 677–681
22. Rinella, M. E., and Green, R. M. (2004) *J. Hepatol.* **40,** 47–51
23. Rizki, G., Arnaboldi, L., Gabrielli, B., Yan, J., Lee, G. S., Ng, R. K., Turner, S. M., Badger, T. M., Pitas, R. E., and Maher, J. J. (2006) *J. Lipid Res.* **47,** 2280–2290
24. Gallegos, L. L., Kunkel, M. T., and Newton, A. C. (2006) *J. Biol. Chem.* **281,** 30947–30956
25. Medkova, M., and Cho, W. (1998) *Biochemistry* **37,** 4892–4900
26. Melowic, H. R., Stahelin, R. V., Blatner, N. R., Tian, W., Hayashi, K., Altman, A., and Cho, W. (2007) *J. Biol. Chem.* **282,** 21467–21476
27. Ohmori, S., Shirai, Y., Sakai, N., Fujii, M., Konishi, H., Kikkawa, U., and Saito, N. (1998) *Mol. Cell. Biol.* **18,** 5263–5271
28. Parekh, D. B., Ziegler, W., and Parker, P. J. (2000) *EMBO J.* **19,** 496–503
29. Ota, T., Gayet, C., and Ginsberg, H. N. (2008) *J. Clin. Invest.* **118,** 316–332
30. Ozcan, U., Cao, Q., Yilmaz, E., Lee, A. H., Iwakoshi, N. N., Ozdelen, E., Tuncman, G., Görgün, C., Glimcher, L. H., and Hotamisligil, G. S. (2004) *Science* **306,** 457–461
31. Ozcan, U., Yilmaz, E., Ozcan, L., Furuhashi, M., Vaillancourt, E., Smith, R. O., Görgün, C. Z., and Hotamisligil, G. S. (2006) *Science* **313,** 1137–1140
32. Pfaffenbach, K. T., Gentile, C. L., Nivala, A. M., Wang, D., Wei, Y., and Pagliassotti, M. J. (2010) *Am. J. Physiol. Endocrinol Metab.* **298,** E1027–E1035
33. Rahman, S. M., Schroeder-Gloeckler, J. M., Janssen, R. C., Jiang, H., Qadri, I., Maclean, K. N., and Friedman, J. E. (2007) *Hepatology* **45,** 1108–1117
34. Hansson, P. K., Asztély, A. K., Clapham, J. C., and Schreyer, S. A. (2004) *Biochim. Biophys. Acta* **1684,** 54–62
35. Kohli, R., Pan, X., Malladi, P., Wainwright, M. S., and Whitington, P. F. (2007) *J. Biol. Chem.* **282,** 21327–21336
36. Sahai, A., Pan, X., Paul, R., Malladi, P., Kohli, R., and Whitington, P. F. (2006) *Am. J. Physiol. Gastrointest. Liver Physiol.* **291,** G55–G62
37. Chang, Y. C., and Oas, T. G. (2010) *Biochemistry* **49,** 5086–5096
38. Lin, S. L., Zarrine-Afsar, A., and Davidson, A. R. (2009) *Protein Sci.* **18,** 526–536
39. Shepshelovich, J., Goldstein-Magal, L., Globerson, A., Yen, P. M., Rotman-Pikielny, P., and Hirschberg, K. (2005) *J. Cell Sci.* **118,** 1577–1586
40. Wei, H., Kim, S. J., Zhang, Z., Tsai, P. C., Wisniewski, K. E., and Mukherjee, A. B. (2008) *Hum. Mol. Genet.* **17,** 469–477
41. Siolas, D., Lerner, C., Burchard, J., Ge, W., Linsley, P. S., Paddison, P. J., Hannon, G. J., and Cleary, M. A. (2005) *Nat. Biotechnol.* **23,** 227–231
42. Leclercq, I. A., Farrell, G. C., Field, J., Bell, D. R., Gonzalez, F. J., and Robertson, G. R. (2000) *J. Clin. Invest.* **105,** 1067–1075
43. Pickens, M. K., Yan, J. S., Ng, R. K., Ogata, H., Grenert, J. P., Beysen, C., Turner, S. M., and Maher, J. J. (2009) *J. Lipid Res.* **50,** 2072–2082
44. Rinella, M. E., Elias, M. S., Smolak, R. R., Fu, T., Borensztajn, J., and Green, R. M. (2008) *J. Lipid Res.* **49,** 1068–1076
45. Samuel, V. T., Liu, Z. X., Qu, X., Elder, B. D., Bilz, S., Befroy, D., Romanelli, A. J., and Shulman, G. I. (2004) *J. Biol. Chem.* **279,** 32345–32353

46. Kammoun, H. L., Chabanon, H., Hainault, I., Luquet, S., Magnan, C., Koike, T., Ferré, P., and Foufelle, F. (2009) *J. Clin. Invest.* **119,** 1201–1215
47. Su, Q., Tsai, J., Xu, E., Qiu, W., Bereczki, E., Santha, M., and Adeli, K. (2009) *Hepatology* **50,** 77–84
48. Wei, Y., Wang, D., Gentile, C. L., and Pagliassotti, M. J. (2009) *Mol. Cell Biochem.* **331,** 31–40
49. Wang, D., Wei, Y., and Pagliassotti, M. J. (2006) *Endocrinology* **147,** 943–951
50. Wei, Y., Wang, D., and Pagliassotti, M. J. (2007) *Mol. Cell Biochem.* **303,** 105–113
51. Wei, Y., Wang, D., Topczewski, F., and Pagliassotti, M. J. (2006) *Am. J. Physiol. Endocrinol. Metab.* **291,** E275–E281
52. Qi, X., Vallentin, A., Churchill, E., and Mochly-Rosen, D. (2007) *J. Mol. Cell. Cardiol.* **43,** 420–428
53. Akazawa, Y., Cazanave, S., Mott, J. L., Elmi, N., Bronk, S. F., Kohno, S., Charlton, M. R., and Gores, G. J. (2010) *J. Hepatol.* **52,** 586–593
54. Ron, D., and Walter, P. (2007) *Nat. Rev. Mol. Cell Biol.* **8,** 519–529
55. Wu, J., and Kaufman, R. J. (2006) *Cell Death Differ.* **13,** 374–384
56. Tamaki, N., Hatano, E., Taura, K., Tada, M., Kodama, Y., Nitta, T., Iwaisako, K., Seo, S., Nakajima, A., Ikai, I., and Uemoto, S. (2008) *Am. J. Physiol. Gastrointest. Liver Physiol.* **294,** G498–G505